CSIAM Trans. Life Sci.
doi: 10.4208/csiam-ls.SO-2025-0029

Vol. **x**, No. x, pp. 1-30
xx 2026

# Markov Chain Modeling Hepatitis B Virus Infection with Liver Microstructure

Haonan Zhong[1], Jinliang Wang[2,*] and Kaifa Wang[1,*]

[1] *School of Mathematics and Statistics, Southwest University, Chongqing 400715, P. R. China.*
[2] *School of Mathematical Science, Heilongjiang University, Harbin 150080, P. R. China.*

Received 17 November 2025; Accepted 12 January 2026

**Abstract.** Based on the special blood supply system and microscopic structure of the liver, a series of novel Markov chain models is constructed to mimic the entire dynamic process of hepatitis B virus colonization, diffusion and evolution in liver, named as colonization Markov chain, diffusion Markov chain and evolution Markov chain. Theoretically, the colonization probability and infection distribution in hepatic lobules are first obtained. Then, the likelihood of sustained chronicity risk and the expected recovery time for chronic hepatitis B patients undergoing antiviral therapy are also derived. Numerical simulations validate the feasibility of models and the theoretical results. Especially, the model of evolutionary Markov chain with immune saturation may be suitable to simulate the clinically observed complex kinetic patterns of biomarkers, which has potential clinical application prospects.

**AMS subject classifications**: 92D30, 92C60

**Key words**: Hepatitis B virus infection, hepatic lobules, Markov chain, sustained chronicity risk, expected recovery time.

## 1 Introduction

Although the World Health Organization (WHO) has set a global target to eliminate viral hepatitis by 2030, hepatitis B remains a considerable public health burden under current interventions [32,34]. Hepatitis B virus (HBV) infection can cause acute or chronic hepatitis [14,22], with 2022 estimates indicating 254 million people living with chronic hepatitis B (CHB) and about 1.2 million new infections annually [39]. Standard treatments for CHB include long-term nucleos(t)ide analogues (NAs) or finite courses of pegylated in-

*Corresponding author. *Email addresses:* jinliangwang@hlju.edu.cn (J. Wang), kfwang72@163.com (K. Wang)

 

terferon alpha (Peg-IFN-$\alpha$) [9,13,23]. However, their efficacy in achieving hepatitis B surface antigen (HBsAg) seroclearance remains debated [41], and functional cure rates are still low [18,42]. Therefore, alongside optimizing therapies and developing new drugs, understanding the risk of sustained chronicity and predicting recovery times under antiviral treatment are also crucial for reaching the WHO's 2030 elimination goal.

In 1996, Nowak *et al.* [29] pioneered a basic three-dimensional ordinary differential equations (ODEs) model to describe host–virus interactions, enabling estimation of infected hepatocyte dynamics and lamivudine efficacy. Subsequent extensions incorporated cytotoxic T lymphocytes (CTLs) responses to analyze immune effects [28] and examined the influence of intracellular viral dynamics on plasma virus decay [12]. Since then, more sophisticated ODEs-based models have been developed to elucidate biological mechanisms during HBV infection and treatment [4,11,25,37]. Now, dynamical models have contributed substantially to optimizing therapeutic strategies and understanding the basis of chronicity [1,8,10,17,19,24]. However, there is a common hypothesis that the hepatocytes are homogeneously distributed in the liver in terms of the viral transmission, i.e. the probability of each hepatocyte being infected is equal, and the hepatocytes are often simply divided into several states, such as infected and uninfected hepatocytes.

In fact, as the largest digestive organ, the liver possesses a unique blood supply and microstructure. It receives blood from both the hepatic artery and portal vein, which then drains through the hepatic vein [26, 30, 35]. Histologically, the hepatic lobule is the basic functional units of liver, each composed of approximately 50,000-100,000 hepatocytes arranged in a hexagonal architecture radiating from the central vein to the peripheral portal triads [3,21,26,35,40]. Due to the hepatotropism of HBV, infection initiates within these lobules, and the direction of blood flow governs the primary colonization path of virions [5,35]. This distinct spatial organization implies that hepatocytes are not homogeneously distributed, thereby challenging the assumption of uniform infection probability used in the existing models.

The hierarchical and directional nature of the liver microstructure provides a strong rationale for applying Markov chains to model HBV infection within the liver. However, to the best of our knowledge, such an approach has not yet been employed in studying HBV infection in vivo. To address the limitation of cellular heterogeneity, we propose three Markov chain models – colonization Markov chain (CMC), diffusion Markov chain (DMC), and evolution Markov chain (EMC) – to systematically characterize the processes of viral colonization, diffusion, and evolution within the liver. This framework not only reveals dynamical features of HBV infection, but also offers a novel methodology for enriching the study of HBV infection within-host.

## 2 HBV colonization within a hepatic lobule

This section formulates a discrete-state colonization Markov chain (CMC) model in details, to depict the colonization process of HBV invading the hepatocyte in a health hep-

atic lobule. According to the CMC model, we estimate the absorption probabilities of an HBV particle, especially the probability of successful colonization. In addition, we investigate the probability distribution by layers under the condition of lobule infected.

## 2.1 Model formulation

We first introduce the process of HBV colonization in a health hepatic lobule. When an HBV particle enters the portal area of hepatic lobules through the bloodstream, it flows with the bloodstream through the extracellular space (hepatic sinusoids). The virion searches for the specific surface receptor on hepatocytes, such as sodium taurocholate cotransporting polypeptide receptor. Upon finding these receptors, the particle binds to it and enters the hepatocytes via endocytosis or fusion, and finally completes the colonization process [36]. If not finding the receptors, it moves inward with the bloodstream and repeats the abovementioned process. Based on the above biological mechanisms, we can conclude that the process of HBV colonization follows the following two key biological facts:

- the movement of viral particles follows the direction of blood flow;
- hepatocytes within hepatic lobules are arranged concentrically around the central vein (CV).

We now begin to establish the CMC model. Based on the abovementioned biological fundamentals, we can denote the center vein and the concentric layers along the radius outward as state $V$ and $1,2,3,\ldots,n$. Then, for a virion at the $k$-th ($k\geq 2$) layer, it has two irreversible results and two free results. The irreversible results are to be neutralized by the immune system and to find the receptor successfully, which are assumed to be independent and have probability $\alpha_n$ for being neutralized and probability $\alpha_r$ for finding and binding to receptors, respectively. The free results are to flow to the inner layer or to stay at the same layer, the probabilities of which are supposed to be $\beta_1$ for the inner layer and $\beta_0\,(\beta_1+\beta_0=1)$ for the same layer, respectively. Particularly, if the virion successfully arrives at the first layer, i.e. the innermost hepatocyte next to the center vein, its irreversible results will be one more than previous states, that is to enter into the CV. Combing the two irreversible results and the layer structure, we can outline all possible results of virions in the lobule. For reading convenience, the transformation map is presented in Fig. 1. The circle $k=1,2,\ldots,n$ denotes the state that the virion is in the hepatic sinusoid outside the hepatocytes at the $k$-th layer, and the circle $V$ denotes the state that the virion enters into the CV. Besides, the circles $C,N$ denote the states that the virion has colonized into the hepatocyte or been neutralized by the immune system, respectively.

Next, we calculate the one-step transition probability among these states. Suppose the virion now is at the state $k\geq 1$, the probability $P_N$ equals to $\alpha_n$, implying it is neutralized by the immune system. The probability $P_C$ is $(1-\alpha_n)\alpha_r$ resulting from the inde-

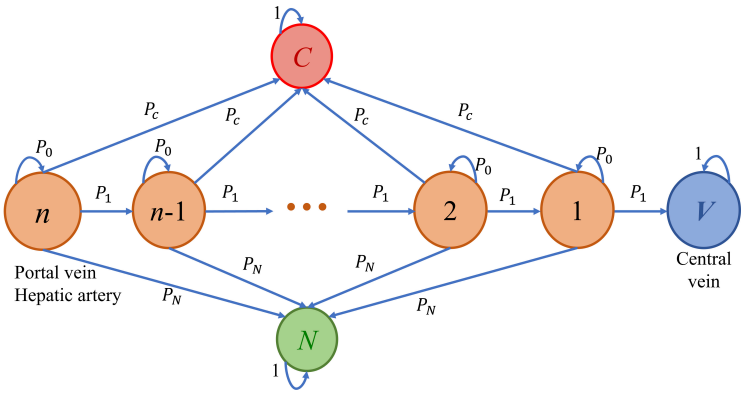


Figure 1: The transformation map of CMC model. States 1,2,...,$n$ represent the virion residing in the extracellular space (sinusoid) at the corresponding layer. States $C, N$, and $V$ represent colonization, neutralization, and entering the CV, respectively. $P_C, P_N$ are the probabilities of successful colonization in the hepatocyte and neutralization, while $P_0, P_1$ are the probabilities of remaining in the same layer or moving inward to the inner layer.

pendence of the two events, i.e. the virion escapes the immune neutralization with probability $1-\alpha_n$ and finds the receptor with probability $\alpha_r$. The probabilities $P_0$ and $P_1$ are $(1-\alpha_n)(1-\alpha_r)\beta_0$ and $(1-\alpha_n)(1-\alpha_r)\beta_1$ since the independence of the three events, i.e. the virion escapes the immune neutralization with probability $(1-\alpha_n)$, fails to find the receptor with probability $(1-\alpha_r)$ and remains at the same layer with probability $\beta_0$ or moves into the inner layer with probability $\beta_1$. For convenience, we put the four one-step transition probabilities in Table 1.

Since a hepatic lobule is around 1-1.4mm in width and a hepatocyte is about 20-30μm in diameter [16,33,40], we can estimate there are around 17-25 hepatocytes on the radius of a lobule, i.e. $n \in \{17,18,\ldots,25\}$. Combining the state transition map in Fig. 1 and the four state transition probability in Table 1, we finally complete the formulation of CMC model.

Table 1: Four one-step transition probabilities of state $k$.

| Definition | Description | Expression |
|---|---|---|
| $P_N$ | Probability of neutralization | $\alpha_n$ |
| $P_C$ | Probability of colonization | $(1-\alpha_n)\alpha_r$ |
| $P_0$ | Probability to state $k$ | $(1-\alpha_n)(1-\alpha_r)\beta_0$ |
| $P_1$ | Probability to state $k-1$ | $(1-\alpha_n)(1-\alpha_r)\beta_1$ |

## 2.2 Absorption probability distribution

The state set of CMC model is $S_{\text{cmc}}=\{N,C,V,1,2,\ldots,n-1,n\}$. Here the states $\{N,C,V\}$ are the absorbing states. To obtain their absorption probabilities, we first define $\mathbb{P}_{\text{cmc}}=\{p_{ij}\}$

as the transition probability matrix with elements $p_{ij}$ denoting the transition probability from state $j$ to state $i$. According to the state order in $S_{\text{cmc}}$, the corresponding one-step transition probability matrix $\mathbb{P}_{\text{cmc}}$ of CMC model can be shown as follows:

$$\mathbb{P}_{\text{cmc}}=\begin{pmatrix}1&0&0&P_N&\cdots&P_N&P_N&P_N&P_N\\0&1&0&P_C&\cdots&P_C&P_C&P_C&P_C\\0&0&1&P_1&\cdots&0&0&0&0\\0&0&0&P_0&\cdots&0&0&0&0\\\vdots&\vdots&\vdots&\vdots&\ddots&\vdots&\vdots&\vdots&\vdots\\0&0&0&0&\cdots&P_0&P_1&0&0\\0&0&0&0&\cdots&0&P_0&P_1&0\\0&0&0&0&\cdots&0&0&P_0&P_1\\0&0&0&0&\cdots&0&0&0&P_0\end{pmatrix}.$$

We now present the method to calculate the absorbing probability. In the transition matrix $\mathbb{P}_{\text{cmc}}$, the states $\{N,C,V\}$ are the absorbing states and the rest states $k\,(1\le k\le n)$ are transient states. For each transient state $k$, we use $P_{Ck},P_{Nk},P_{Vk}$ to denote the absorbing probabilities from the transient state $k$ to the absorbing states $\{C,N,V\}$, respectively. Taking $P_{Ck}$ as an example, its expression can be derived as following operations. From Fig. 1, the probability $P_{Ck}$ contains three different parts. The first part is the direct absorbing probability $P_C$ denoting flowing into state $C$ with probability $P_C$. The second part is the indirect absorbing probability $P_0\times P_{Ck}$ denoting flowing into itself with probability $P_0$ and still having its own absorbing probability $P_{Ck}$. The third part is also the indirect absorbing probability $P_1\times P_{C(k-1)}$ denoting flowing into state $k-1$ with probability $P_1$ and having the absorbing probability $P_{C(k-1)}$. Thus, the absorbing probability $P_{Ck}$ from state $k$ to $C$ can be expressed by the following difference equation:

$$P_{Ck}=P_C+P_0\times P_{Ck}+P_1\times P_{C(k-1)},\quad 1\le k\le n. \tag{2.1}$$

Eq. (2.1) is a first-order difference equation of $P_{Ck}$, which can be rewritten as

$$P_{Ck}=\frac{P_1}{1-P_0}P_{C,k-1}+\frac{P_C}{1-P_0},\quad k=1,\ldots,n.$$

Particularly, for the initial condition $k=1$, we have

$$P_{C1}=\frac{P_1}{1-P_0}P_{CV}+\frac{P_C}{1-P_0}=\frac{P_C}{1-P_0}.$$

Because the state $V$ is an absorbing state, implying it is impossible to switch from state $V$ to state $C$, i.e. $P_{CV}=0$. As a result, the general term of $P_{Ck}$ can be solved by iterations, which are

$$P_{Ck}=\frac{P_C}{1-P_0-P_1}\left[1-\left(\frac{P_1}{1-P_0}\right)^k\right],\quad k=1,2,\ldots,n.$$

Since $P_C+P_N+P_1+P_0=1$, we have

$$P_{Ck}=\frac{P_C}{P_C+P_N}\left[1-\left(\frac{P_1}{1-P_0}\right)^k\right],\quad k=1,2,\ldots,n. \tag{2.2}$$

Similarly, we can get the recursive expressions of $P_{Nk}$ and $P_{Vk}$

$$\begin{cases} P_{Nk}=P_N+P_0P_{Nk}+P_1P_{N(k-1)},\\ P_{Vk}=P_0P_{Vk}+P_1P_{V(k-1)} \end{cases} \tag{2.3}$$

for $1\leq k\leq n$ with the boundary conditions

$$P_{N1}=\frac{P_N}{1-P_0},\quad P_{V1}=\frac{P_1}{1-P_0},$$

because of $P_{NV}=0, P_{VV}=1$. Similarly, Eqs. (2.3) can be solved by iterations, which are

$$P_{Nk}=\frac{P_N}{P_C+P_N}\left[1-\left(\frac{P_1}{1-P_0}\right)^k\right],\quad P_{Vk}=\left(\frac{P_1}{1-P_0}\right)^k,\quad k=1,2,\ldots,n. \tag{2.4}$$

From (2.2) and (2.4), we obtain the three absorbing probabilities $P_{Ck},P_{Nk},P_{Vk}$ from the transient state $k$, which are concluded in the following proposition.

**Proposition 2.1.** *The absorbing probability distribution of states $\{C,N,V\}$ from state k in CMC model are*

$$(P_{Ck},P_{Nk},P_{Vk})=\left(\frac{P_C}{P_C+P_N}(1-\bar{P}_1^k),\frac{P_N}{P_C+P_N}(1-\bar{P}_1^k),\bar{P}_1^k\right),\quad k=1,\ldots,n, \tag{2.5}$$

*where $\bar{P}_1:=P_1/(1-P_0)$.*

From Proposition 2.1, we can quickly obtain the first colonization probability by an invading HBV particle for a health hepatic lobule. We view a hepatic lobule as colonized if there exists at least one colonized hepatocyte in the lobule. Let $\mathscr{C}$ denote the events of successful colonization by HBV particle after the first HBV particle enters into the hepatic lobule. Considering the HBV particle enters into the lobule from the outmost layer (the $n$-th layer), the first colonization probability $\mathbb{P}(\mathscr{C})$ should be

$$\mathbb{P}(\mathscr{C})=\frac{P_C}{P_C+P_N}(1-\bar{P}_1^n). \tag{2.6}$$

## 2.3 Layer-wise colonization probability distribution

The previous subsection demonstrated that colonization probability varies across different layers. This section will investigate the corresponding conditional probability for

each layer, given that the hepatic lobule is colonized. The conditional probability provides a quantitative measure of the infection risk for each individual layer.

Denote $\mathscr{F}_k$ as the event that hepatocyte at the $k$-th layer is infected, then the conditional probability should be $\mathbb{P}_{\text{dis}}(k)=\text{Prob}(\mathscr{F}_k|\mathscr{C}), k=1,2,\ldots,n$. Since $\mathscr{F}_k\subset\mathscr{C}$, we have

$$\mathbb{P}_{\text{dis}}(k)=\frac{\text{Prob}(\mathscr{F}_k)}{\mathbb{P}(\mathscr{C})}. \tag{2.7}$$

Since $\mathbb{P}(\mathscr{C})$ is known in (2.6), we next find $\text{Prob}(\mathscr{F}_k)$. $\text{Prob}(\mathscr{F}_k)$ depends on two events. The first event is that the virion can move inward to the $k$-th layer from the outmost layer, the probability of which is denoted as $\mathbb{P}_{\text{m}}(k)$ and the second event is that the virion can colonize the hepatocyte while at the $k$-th layer, the probability of which is denoted as $\bar{P}_C$.

Subsequently, we consider the probability of virions moving one layer inward, which includes two events that the virion moves to the inner layer directly or after staying at the current layer for some transition steps. It can be viewed as a cumulative probability of one-step transition probability $P_1$ and expressed as follows:

$$\sum_{i=0}^{+\infty}P_0^iP_1=\frac{P_1}{1-P_0}=\bar{P}_1.$$

Thus, the probability $\mathbb{P}_{\text{m}}(k)=\bar{P}_1^{n-k}$. Similarly, $\bar{P}_C$ includes two events that the virion invades into the hepatocyte directly or after staying at the current layer for some transition steps, which is also the cumulative probability of one-step transition probability $P_C$ with expression as follows:

$$\bar{P}_C=\sum_{i=0}^{+\infty}P_0^iP_C=\frac{P_C}{1-P_0}. \tag{2.8}$$

Combining $\mathbb{P}_{\text{m}}(k)$ and $\bar{P}_C$, we have $\text{Prob}(\mathscr{F}_k)=\bar{P}_C\bar{P}_1^{n-k}$. Thus, the colonization probability $\mathbb{P}_{\text{dis}}(k)$ can be concluded in the following proposition.

**Proposition 2.2.** *The layer-wise colonization probability distribution $\mathbb{P}_{\text{dis}}(k)$ is a discrete exponential distribution, satisfying*

$$\mathbb{P}_{\text{dis}}(k)=\frac{\bar{P}_C\bar{P}_1^n}{1-\bar{P}_1^n}\left(1+\frac{P_N}{P_C}\right)\bar{P}_1^{-k},\quad k=1,\ldots,n, \tag{2.9}$$

*and the outmost layer has the maximum probability to be colonized.*

## 3 HBV diffusion within a hepatic lobule

This section introduces the infection diffusion process within a hepatic lobule and proposes a diffusion Markov chain model to measure it. Based on this model, we analyze the probability distribution of the size of infected hepatocytes and derive its expectation and variance.

### 3.1 Model formulation

During the early stage of HBV diffusion within an infected hepatic lobule, because cytolytic effect is not activated, the host is unvaccinated and lacks specific immunity. In addition, since hepatocytes are long-lived cells, infected hepatocytes can alive and productive for a considerable period. Furthermore, after a virion colonizes a hepatocyte, its relaxed circular DNA is converted to the covalently closed circular DNA (cccDNA) in the nucleus, which serves as the template for new viruses [11,36]. The cccDNA transcribes pregenomic RNA, which is then reverse-transcribed into single-stranded DNA and double-stranded DNA (dsDNA) [11,36]. Thus, considering the release of a dsDNA particle as the initiation of a new infection diffusion, we further conclude that at most one progeny virion can be released from the infection site, and the release of more than one particle is impossible during a sufficient small time interval $\Delta t$. As a result, the following two plausible biological facts can be summarized as follows:

- the DMC model is considered as a birth process;
- at most one progeny virion can be released from the infection site during $\Delta t$.

We now formulate the DMC model. Suppose the hepatocyte at the $k$-th layer is the original infected cell, denote $x(t)$ as the number of infected hepatocytes in the infected lobule at time $t$ and $x(0)=1$, and let $p_{i+j,i}(\Delta t)$ be the infinitesimal transition probability from state $x(t)=i, i\in\mathbb{Z}_+$ to $x(t+\Delta t)=i+j, j\in\mathbb{Z}$ in a sufficient small $\Delta t$, which is also the probability of the increment $\Delta x(t)=x(t+\Delta t)-x(t)$, satisfying

$$p_{i+j,i}(\Delta t)=\text{Prob}\big(\Delta x(t)=j|x(t)=i\big).$$

We next present the possible states of $\Delta x(t)=j, j\in\mathbb{Z}$. From the abovementioned first biological fact, the DMC is viewed as a birth process, implying the probability $p_{i+j,i}(\Delta t)=0$ for $j<0$. From the second biological fact mentioned above, the probability $p_{i+j,i}(\Delta t)$ of $j\geq 2$ should faster converge to 0 than that of $\Delta t$, i.e. $p_{i+j,i}(\Delta t)=o(\Delta t), j\geq 2$. As for the states of $j=0,1$, we only discuss the case of $j=1$ since they are complementary. Generally, the transition probability not only relies on the time interval $\Delta t$, but also depends on the number of infected cells $x(t)$, which can be expressed as follows:

$$p_{i+1,i}(\Delta t)=f\big(x(t)\big)\Delta t+o(\Delta t),\quad p_{i,i}(\Delta t)=1-f\big(x(t)\big)\Delta t+o(\Delta t),$$

where $f(x(t))$ is the force function contributed by each infected hepatocyte. Taken together, the transition probabilities of DMC model can be described as follows:

$$\begin{aligned} p_{i+j,i}(\Delta t)&=\text{Prob}\big(\Delta x(t)=j\,|\,x(t)=i\big)\\ &=\begin{cases} f(i)\Delta t+o(\Delta t), & j=1,\\ 1-f(i)\Delta t+o(\Delta t), & j=0,\\ o(\Delta t), & j\geq 2,\\ 0, & j<0. \end{cases} \end{aligned} \tag{3.1}$$

It is critical to determine the force function $f(x)$ in (3.1), since it not only reflects the infection patterns of HBV, but also binds the DMC model and HBV infection together.

The determination of the force function $f(x)$ is based on two key factors: transmission channels and growth patterns. We begin with discussion of the transmission channels. Unlike the infection process during the colonization stage, the infection pattern during the diffusion process involves not only cell-to-virus transmission but also cell-to-cell transmission [11,43,44]. Due to the opposing flow directions of bile and bloodstream, it is possible for virions to travel with the bile and infect hepatocytes in the outer layers. However, the bile canaliculus as one of the intercellualr space, is quite tight and narrow [31, 36], which is illustrated in Fig. 2. Thus, we categorize the transmission by bile canaliculus into the cell-to-cell transmission. Besides the bile canaliculus, it is well-known that the hepatocyte is highly polarized because of the existence of the cell connecting surface including the tight junction, desmosomes and the gap junction, which contributes to the cell-to-cell transmission as well [36,43,44].

As a result, the cell-to-cell transmission is necessarily incorporated into the force function $f(x)$. Taking the hepatocyte at the $k$-th layer as an example, and assuming the release probabilities of a progeny through cell-to-cell transmission and cell-to-virus transmission are $P_{\rm cc}$ and $P_{\rm cv}$ $(P_{\rm cc}+P_{\rm cv}=1)$ respectively, and thus, the probability increment contributed should be

$$r_k := P_{\rm cc}+P_{\rm cv}P_{Ck},$$

where $P_{Ck}$ is defined in (2.2). Furthermore, supposing the proportion of hepatocytes in each layer merely depends on the order of layers, the mean probability increment in a hepatocyte is

$$r=\sum_{k=1}^{n}\frac{k}{\sum_{i=1}^{n}i}r_k=P_{\rm cc}+\frac{2P_{\rm cv}}{n^2+n}\sum_{k=1}^{n}kP_{Ck}.$$

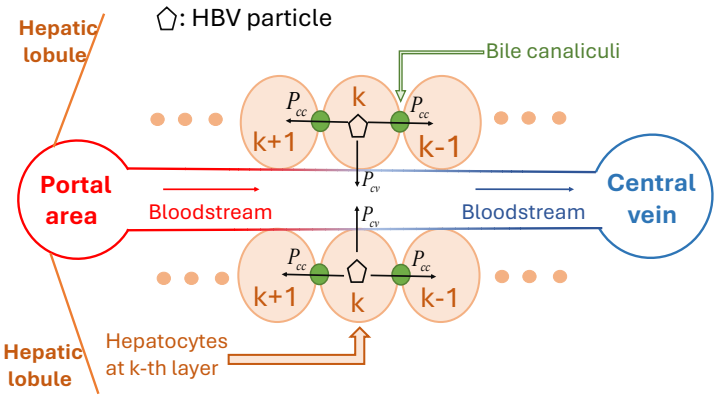


Figure 2: Illustration of two transmission channels of HBV particle diffusion. The release probability of HBV particle containing dsDNA through cell-to-cell transmission is $P_{\rm cc}$, and the release probability of HBV particle containing dsDNA through cell-to-virus transmission is $P_{\rm cv}$ $(P_{\rm cc}+P_{\rm cv}=1)$.

We next discuss the growth pattern of the infection diffusion process. First, all classical force functions $f(x)$ in (3.1) must meet the three basic conditions: nonnegativity, boundedness and $f(0)=f(x)=0$ as $x\geq K$. Here, $K$ is the hepatocyte capacity of a hepatic lobule. Additionally, the most common functional forms used to describe growth patterns are the linear and logistic forms. Therefore, the force function $f(x)$ can be expressed as follows:

$$f_{\ln}(x)\triangleq\begin{cases} rx, & 0\leq x<K,\\ 0, & x\geq K,\end{cases}\quad\text{and}\quad f_{\lg}(x)\triangleq\begin{cases} rx\left(1-\dfrac{x}{K}\right), & 0\leq x<K,\\ 0, & x\geq K.\end{cases}\tag{3.2}$$

### 3.2 Probability distribution of DMC model with general force function

Since DMC is a continuous-time Markov chain, we can investigate its state classification through the discrete embedded Markov chain, which is

$$\mathbb{T}_{\mathrm{DMC}}=\begin{pmatrix} 0 & 0 & 0 & \cdots & 0 & 0 & 0\\ 0 & 0 & 0 & \cdots & 0 & 0 & 0\\ 0 & 1 & 0 & \cdots & 0 & 0 & 0\\ \vdots & \vdots & \vdots & \ddots & \vdots & \vdots & \vdots\\ 0 & 0 & 0 & \cdots & 0 & 0 & 0\\ 0 & 0 & 0 & \cdots & 1 & 0 & 0\\ 0 & 0 & 0 & \cdots & 0 & 1 & 0\end{pmatrix}.$$

From the embedded Markov chain, the state transition map can be drawn as

$$\{0\},\quad \{1\to 2\to 3\to\cdots\to K-1\to K\}.$$

Thus, $\{0\}$ is an isolated closed state, $\{1,2,\ldots,K-1\}$ is the transient open class, and the capacity $K$ is the unique absorption state, implying

$$\mathrm{Prob}\big(x(t)=K\big)=1,\quad \text{as}\quad t\ \to\ +\infty.\tag{3.3}$$

Thus, from the boundedness of $x(t)$, the expectation and variance of $x(t)$ satisfy $\mathbb{E}(x(t))=K,\mathbb{V}\mathrm{ar}(x(t))=0$, as $t\to+\infty$. It indicates that the stochastic solution of DMC model almost surely converges to the capacity $K$, further implying

$$\mathbb{E}\big(x(t)^n\big)=\mathbb{E}^n\big(x(t)\big)=K^n,\quad n\in\mathbb{Z}_+,\quad \text{as}\quad t\ \to\ +\infty.\tag{3.4}$$

We next investigate the probability distribution of DMC model with general force function $f(x)$. For concise notations, denote $f(i)=f_i$ and let $p_i(t)$ be the probability of $x(t)=i$ at time $t$, then $p_i(t+\Delta t)$ meets the following equation:

$$p_i(t+\Delta t)=p_{i,i-1}(\Delta t)p_{i-1}(t)+p_{i,i}(\Delta t)p_i(t).$$

Based on (3.1), we can get the following recurrence equation in a small $\Delta t$:

$$p_i(t+\Delta t) = f_{i-1}\Delta t \cdot p_{i-1}(t) + (1 - f_i \Delta t) \cdot p_i(t),$$

and further obtain the corresponding forward Kolmogorov differential equation

$$\begin{cases} \dfrac{\mathrm{d}p_i(t)}{\mathrm{d}t} = f_{i-1}p_{i-1}(t) - f_i p_i(t), \quad i \geq 2, & \text{(3.5a)} \\ \dfrac{\mathrm{d}p_1(t)}{\mathrm{d}t} = -f_1 p_1(t), \quad p_1(0) = 1. & \text{(3.5b)} \end{cases}$$

By multiplying $\exp(-f_i t)$ on the both sides of the Eq. (3.5a), we can get the following iteration algorithm:

$$p_i(t) = p_i(0)e^{-f_i t} + f_{i-1}\int_0^t e^{-f_i(t-s)} p_{i-1}(s)ds, \quad i \in \mathbb{Z}_+.$$

Combining with the Eq. (3.5b) and considering $p_1(0) = 1$ and $p_i(0) = 0, i \geq 2$, we have the following recurrence formulae:

$$\begin{cases} p_1(t) = e^{-f_1 t}, \\ p_i(t) = f_{i-1}\displaystyle\int_0^t e^{-f_i(t-s)} p_{i-1}(s)ds, \quad i \geq 2. \end{cases}$$

After some computations, we have

$$\begin{aligned} &p_1(t) = e^{-f_1 t}, \quad p_2(t) = f_1\left[\frac{e^{-f_1 t}}{f_2 - f_1} + \frac{e^{-f_2 t}}{f_1 - f_2}\right], \\ &p_3(t) = f_1 f_2\left[\frac{e^{-f_1 t}}{(f_2 - f_1)(f_3 - f_1)} + \frac{e^{-f_2 t}}{(f_1 - f_2)(f_3 - f_2)} + \frac{e^{-f_3 t}}{(f_1 - f_3)(f_2 - f_3)}\right]. \end{aligned}$$

Based on the inductive method, we finally obtain the solution of $p_i(t)$ as follows:

$$p_i(t) = \prod_{j=1}^{i-1} f_j \cdot \left[\sum_{j=1}^{i}\prod_{k\neq j}^{i}(f_k - f_j)^{-1} e^{-f_j t}\right]. \tag{3.6}$$

It is feasible to obtain the analytical solution of $p_i(t)$ and the expectation and variance based on (3.6) when the capacity $K$ is small or the force function $f(x)$ has an appropriate structure. More generally, the expectation and variance of $x(t)$ at least can be obtained by definition and calculated by computers, i.e.

$$\mathbb{E}\big(x(t)\big) = \sum_{i=0}^{+\infty} i p_i(t), \quad \mathbb{E}\big(x^2(t)\big) = \sum_{i=0}^{+\infty} i^2 p_i(t), \quad \mathbb{V}\mathrm{ar}\big(x(t)\big) = \mathbb{E}\big(x^2(t)\big) - \mathbb{E}^2\big(x(t)\big).$$

### 3.3 Moment approximation of DMC model with linear force function

Taking $f_{\ln}(x)$ in (3.2) as the force function, the DMC model simplifies to a basic birth process. It implies each hepatocyte independently contributes an increment to the infinitesimal transition probability $p_{i+j,i}(\Delta t)$. The linear growth of $f_{\ln}(x)$ works well to reflect reality as $x(t)$ or $t$ is small, but gradually loses its validity as $x(t)$ becomes larger. Nonetheless, the DMC model with $f_{\ln}(x)$ can be solved analytically, allowing its probability distribution, expectation, and variance to be obtained, which provides valuable references for more complex cases.

We next investigate the influence of $f_{\ln}(x)$ on the DMC model. As $1 \le x(t) \le K-1$ and for a sufficiently small $\Delta t$, the transition probabilities of DMC model are specified as follows:

$$\begin{aligned} p_{i+j,i}(\Delta t) &= \mathrm{Prob}\big(\Delta X(t)=j \,|\, X(t)=i\big) \\ &= \begin{cases} rx(t)\Delta t + \mathrm{o}(\Delta t), & j=1, \\ 1-rx(t)\Delta t + \mathrm{o}(\Delta t), & j=0, \\ \mathrm{o}(\Delta t), & j\ge 2, \\ 0, & j<0. \end{cases} \end{aligned} \tag{3.7}$$

Similar to (3.5), a recurrence system of forward Kolmogorov differential equations can be induced and shown as follows:

$$\begin{cases} \dfrac{\mathrm{d}p_i(t)}{\mathrm{d}t} = r(i-1)p_{i-1}(t) - rip_i(t), & \text{(3.8a)} \\ \dfrac{\mathrm{d}p_1(t)}{\mathrm{d}t} = -rp_1(t), \quad p_1(0)=1, & \text{(3.8b)} \end{cases}$$

where $p_i(t)$ denotes the probability of $x(t)=i, 1 \le i < K$ at time $t$. It is feasible to find an approximated solution of (3.8) by using the generating function technique. In the light of the Eq. (3.8a), multiplying $z^i$ on the both sides and summing over $i$, we obtain

$$\begin{aligned} \frac{\partial}{\partial t}\sum_{i=1}^{+\infty} z^i p_i(t) &= r\sum_{i=1}^{+\infty}(i-1)z^i p_{i-1}(t) - r\sum_{i=1}^{+\infty} iz^i p_i(t) \\ &= rz^2\sum_{i=1}^{+\infty}(i-1)z^{i-2}p_{i-1}(t) - rz\sum_{i=1}^{+\infty} iz^{i-1}p_i(t) \\ &= rz^2\frac{\partial}{\partial z}\sum_{i=1}^{+\infty} z^{i-1}p_{i-1}(t) - rz\frac{\partial}{\partial z}\sum_{i=1}^{+\infty} z^i p_i(t). \end{aligned} \tag{3.9}$$

It can be expressed as the form of partial differential equations

$$\frac{\partial \mathcal{P}(z,t)}{\partial t} = rz^2\frac{\partial \mathcal{P}(z,t)}{\partial z} - rz\frac{\partial \mathcal{P}(z,t)}{\partial z} = rz(z-1)\frac{\partial \mathcal{P}(z,t)}{\partial z}, \quad \mathcal{P}(z,t) = \sum_{i=1}^{+\infty} z^i p_i(t), \tag{3.10}$$

where the domain of $z$ consists of the value that makes $\mathcal{P}(z,t)$ converge. The initial condition for (3.10) is $\mathcal{P}(z,0)=z$. Let $z=e^{\theta}$ and $\mathcal{P}(e^{\theta},t)=M(\theta,t)$, we have

$$\frac{\partial \mathcal{P}(z,t)}{\partial z}=\frac{\partial M(\theta,t)}{\partial z}=\frac{\partial M(\theta,t)}{\partial \theta}\frac{d\theta}{dz}=\frac{1}{z}\frac{\partial M(\theta,t)}{\partial \theta}.$$

Thus, (3.10) can be rewritten as

$$\frac{\partial M}{\partial t}+r(1-e^{\theta})\frac{\partial M}{\partial \theta}=0$$

with initial condition $M(\theta,0)=e^{\theta}$. Thus, we get a first-order linear homogeneous partial differential equation, and it can be solved by the method of characteristics curve [7, 15]. The solution of $M(\theta,t)$ is presented as follows:

$$M(\theta,t)=\frac{1}{1-(1-e^{-\theta})e^{rt}}.$$

Let $\theta=\ln z$ and from $M(\theta,t)$, we can get

$$\mathcal{P}(z,t)=\frac{e^{-rt}z}{1-(1-e^{-rt})z}. \tag{3.11}$$

On the other hand, from the differential equation (3.8b), we have $p_1(t)=\exp(-rt)$. Noticing (3.11) can be expressed by $p_1(t)$, we have

$$\mathcal{P}(z,t)=\frac{p_1 z}{1-(1-p_1)z}=p_1 z\sum_{i=0}^{+\infty}p_1(1-p_1)^i z^i=\sum_{i=1}^{+\infty}p_1(1-p_1)^{i-1}z^i.$$

From the structure of generating probability function $\mathcal{P}(z,t)$, the probability function of $x(t)=i$ with respect to time can be given as follows:

$$p_i(t)=p_1(1-p_1)^{i-1}=e^{-rt}[1-e^{-rt}]^{i-1},\quad i\in\mathbb{Z}_+. \tag{3.12}$$

Since $M(\theta,t)$ is a moment generating function and according to the properties of $M(\theta,t)$, the expectation and variance functions of $x(t)$ can be concluded in the following theorem.

**Theorem 3.1.** *The early infection diffusion process within a hepatic lobule is an exponential increase, i.e. the expectation and variance of $x(t)$ in DMC model with linear force function $f_{\ln}(x)$ admits*

$$\mathbb{E}\big(x(t)\big)=\left.\frac{\partial M(\theta,t)}{\partial \theta}\right|_{\theta=0}=e^{rt},\quad \mathbb{V}\mathrm{ar}\big(x(t)\big)=\mathbb{E}\big(x^2(t)\big)-\mathbb{E}^2\big(x(t)\big)=e^{2rt}-e^{rt}. \tag{3.13}$$

Although we obtain the analytical expressions of moment of $x(t)$, it should be noted that (3.12) and (3.13) are merely valid as $x(t)$ is small, since $f_{\ln}(x)$ for $x\geq K$ is not valid when using moment-generating function methods. Nevertheless, as shown in (3.12) and (3.13), in the early infection diffusion process, the expected infection growth and its variance are anticipated to increase exponentially over time.

### 3.4 Moment analysis of DMC model with logistic force function

The prior linear assumption, which requires independent contributions from each infected hepatocyte, fails as $x(t)$ grows and the fraction of healthy hepatocytes declines. This necessitates the introduction of the logistic force function $f_{\text{lg}}(x)$ in (3.2). However, this adjustment renders analytical solutions intractable. We therefore turn to a qualitative analysis of the expectation and variance of $x(t)$ in this case.

Similarly, the partial differential equation of its moment generating function changes as

$$\frac{\partial M}{\partial t}+r(1-e^{\theta})\left[\frac{\partial M}{\partial \theta}-\frac{1}{K}\frac{\partial^2 M}{\partial \theta^2}\right]=0. \tag{3.14}$$

Differentiating (3.14) with respect to $\theta$ and taking values at $\theta=0$, we have $\mathbb{E}(x^n)=\partial^n M/\partial\theta^n|_{\theta=0}$, and obtain its first and second moments

$$\frac{\mathrm{d}\mathbb{E}(x)}{\mathrm{d}t}=r\mathbb{E}(x)-\frac{r}{K}\mathbb{E}(x^2), \tag{3.15a}$$

$$\frac{\mathrm{d}\mathbb{E}(x^2)}{\mathrm{d}t}=r\mathbb{E}(x)+r\left(2-\frac{1}{K}\right)\mathbb{E}(x^2)-\frac{2r}{K}\mathbb{E}(x^3). \tag{3.15b}$$

Assuming the initial condition $x(0)=k$, i.e. $\text{Prob}\{x(0)=k\}=1$, $k\in[0,K]\cap\mathbb{Z}$, and the assumption further indicates the initial value of (3.15) satisfies

$$\mathbb{E}\big(x(0)\big)=k,\quad \mathbb{V}\text{ar}\big(x(0)\big)=0,\quad \mathbb{E}\big(x(0)^n\big)=\mathbb{E}^n\big(x(0)\big)=k^n. \tag{3.16}$$

From the Eq. (3.15a), we can find that there exists a small $t_0$ such that the expectation $\mathbb{E}(x(t))$ increases over the interval $[0,t_0]$. Besides, considering $\mathbb{V}\text{ar}(x)\geq 0$, we have $\mathbb{E}(x^2)\geq\mathbb{E}^2(x)$. Since $\mathbb{E}(x)>0$, the Eq. (3.15a) can be changed as

$$\frac{\mathrm{d}\mathbb{E}(x)}{\mathrm{d}t}\leq r\mathbb{E}(x)\left[1-\frac{\mathbb{E}(x)}{K}\right]. \tag{3.17}$$

From (3.17), the expectation of DMC model is lower than the deterministic logistic model. Besides, the Eq. (3.15a) can be rewritten as by multiplying $2\mathbb{E}(x)$ on both sides

$$\frac{\mathrm{d}\mathbb{E}^2(x)}{\mathrm{d}t}=2r\mathbb{E}^2(x)-\frac{2r}{K}\mathbb{E}(x^2)\mathbb{E}(x).$$

Combining the Eq. (3.15b), we obtain the differential equation of variance

$$\frac{\mathrm{d}\mathbb{V}\text{ar}(x)}{\mathrm{d}t}=r\mathbb{E}(x)+2r\mathbb{V}\text{ar}(x)-\frac{r}{K}\left[\mathbb{E}(x^2)+2\big(\mathbb{E}(x^3)-\mathbb{E}(x^2)\mathbb{E}(x)\big)\right]. \tag{3.18}$$

From the initial conditions (3.16), since the initial value $x(0)=k<K$, there exists a small $t_0$ such that the variance $\mathbb{V}\text{ar}_t(x)$ increases first over the interval $[0,t_0]$. Besides that, $\mathbb{V}\text{ar}(x)$ increases faster as $r$ or $K$ gets bigger.

We next consider the ultimate states of $\mathbb{E}(x(t))$ and $\mathbb{V}\mathrm{ar}(x(t))$. Recalling the result in (3.4), the convergence of moments further implies the derivative of moments satisfies

$$\lim_{t\to+\infty}\frac{\mathrm{d}\mathbb{E}(x^n)}{\mathrm{d}t}=0. \tag{3.19}$$

If we take the limit state (3.4) back into (3.15), the right sides of the two equations become 0, i.e. $(\mathbb{E}(x(t)),\mathbb{E}(x(t)^2)=(K,K^2)$ is the root of (3.15), which implies all sample paths will finally converge to $x(t)=K$. This finding has a good compatibility with the state classification results in (3.3), that $K$ is an absorbing state.

Finally, we can conclude the moment analysis results in the following theorem.

**Theorem 3.2.** *For long-term infection diffusion process within a hepatic lobule, if the DMC model has a logistic force function, then $\mathbb{E}(x(t))$ will increase first and finally converges to the capacity $K$; $\mathbb{V}\mathrm{ar}(x(t))$ will increase first and finally decrease to 0, implying $K$ is the unique absorbing state.*

# 4 Dynamical evolution of HBV infection among hepatic lobules

This section will study the dynamical evolution of HBV infection among hepatic lobules and introduce the formulation of evolution Markov chain model. Based on the model, we will investigate the sustained chronic risk of HBV infection and the expected recovery time under antiviral therapy.

## 4.1 Model formulation

Assuming that the infection dynamics among hepatic lobules exhibit the Markov property, and let $x(t)$ denote the number of infected lobules at time $t$, we begin by defining the infinitesimal transition probability $p_{i+j,i}(\Delta t)$ of the EMC model as

$$p_{i+j,i}(\Delta t)=\mathrm{Prob}\{x(t+\Delta t)=i+j|x(t)=i\},\quad i\in\mathbb{Z}^+,\quad j\in\mathbb{Z}.$$

Furthermore, it is reasonable to assume that during a sufficiently short interval $\Delta t$, at most one event (a new infection or a recovery) can occur, restricting the possible increment $j$ to the set $J=\{0,1,-1\}$.

We first study the scenario of $j=1$, which includes two distinct infection patterns. The first pattern is the subsequent infection, facilitated by the hepatic lobule's blood supply architecture, wherein multiple lobules share a common interlobular vessel. This structure implies that once the outermost hepatocyte of an upstream lobule is infected, progeny virions can be carried downstream to invade adjacent lobules. The colonization probability for this pattern is given by

$$F_{\mathrm{sub}}(i)\triangleq i\mathbb{P}_{\mathrm{dist}}(n)P_{\mathrm{out}}\left(1-\frac{i}{N}\right)\mathbb{P}(\mathscr{C}),$$

where $\mathbb{P}_{\text{dist}}(n)$, defined in (2.7), is the probability of the outermost hepatocyte being infected, making $i\mathbb{P}_{\text{dist}}(n)$ the estimated number of such lobules. The parameter $P_{\text{out}}$ is the probability that an HBV particle is secreted into the interlobular vein (artery) by an outermost hepatocyte and flows downstream. $(1-i/N)$ represents the proportion of uninfected lobules and $\mathbb{P}(\mathscr{C})$, defined in (2.6), is the probability of successful invasion. By incorporating Eqs. (2.7) and (2.8), we have

$$F_{\text{sub}}(i)=i\bar{P}_C P_{\text{out}}\left(1-\frac{i}{N}\right).$$

The second pattern is blood circulation infection. Suppose each infected lobule releases a mean of $V_{\text{m}}$ virions into circulation and a fraction $P_{\text{res}}$ of these particles survive one complete cycle. Then following the idea of $F_{\text{sub}}$, the corresponding colonization probability is given by

$$F_{\text{cyc}}(i)\triangleq iV_{\text{m}}P_{\text{res}}\left(1-\frac{i}{N}\right)\mathbb{P}(\mathscr{C}).$$

Next, we consider the scenario of $j=-1$, which is governed by two immunity mechanisms. The first is the innate immunity, which is mediated by natural killer (NK) cells. We assume the concentration $c_1$ and the viral clearance rate per contact $r_1$ for NK cells are independent of $x(t)$. Given a bilinear contact rate $k_1c_1i$, where $k_1$ is the unit contact rate, the resulting immune effect function is given as

$$H_{\text{nk}}(i)\triangleq r_1k_1c_1i.$$

The second is driven by specific immunity from cytotoxic T lymphocytes. In contrast to NK cells, the CTL concentration is assumed to scale with the infection burden, denoted as $c_2i$, where $c_2$ quantifies the dependence. With a viral clearance rate $r_2$ per contact and a bilinear contact rate formulated as $k_2c_2i\cdot i$, the specific immune effect function is expressed as

$$H_{\text{ctl}}(i)\triangleq r_2k_2c_2i^2.$$

Based on the abovementioned four equations, the infinitesimal transition probability of the EMC model is given as follows:

$$p_{i+j,i}(\Delta t)=\begin{cases}F_i\Delta t+o(\Delta t), & j=1,\\ H_i\Delta t+o(\Delta t), & j=-1,\\ 1-[F_i+H_i]\Delta t+o(\Delta t), & j=0,\\ o(\Delta t), & j\neq -1,0,1,\end{cases} \tag{4.1}$$

where

$$F_i=F_{\text{sub}}(i)+F_{\text{cyc}}(i),\quad H_i=H_{\text{nk}}(i)+H_{\text{ctl}}(i). \tag{4.2}$$

### 4.2 Moment analyses of EMC model

Similar to the DMC model, the embedded discrete Markov chain of the EMC model is given by

$$\mathbb{T}_{\text{EMC}}=\begin{pmatrix}0 & \mathcal{H}_1 & 0 & \cdots & 0 & 0 & 0\\ 0 & 0 & \mathcal{H}_2 & \cdots & 0 & 0 & 0\\ 0 & \mathcal{F}_1 & 0 & \cdots & 0 & 0 & 0\\ \vdots & \vdots & \vdots & \ddots & \vdots & \vdots & \vdots\\ 0 & 0 & 0 & \cdots & 0 & \mathcal{H}_{N-1} & 0\\ 0 & 0 & 0 & \cdots & \mathcal{F}_{N-2} & 0 & 1\\ 0 & 0 & 0 & \cdots & 0 & \mathcal{F}_{N-1} & 0\end{pmatrix},$$

where

$$\mathcal{H}_i=\frac{H_i}{H_i+F_i},\quad \mathcal{F}_i=\frac{F_i}{H_i+F_i},\quad i=1,\ldots,N-1. \tag{4.3}$$

Subsequently, its state transition map can be drawn as

$$\{0\leftarrow 1\leftrightarrows 2\leftrightarrows 3\leftrightarrows\cdots\leftrightarrows N-1\leftrightarrows N\}.$$

Thus, $\{1,2,\ldots,N\}$ is the transient communication class and 0 is the unique absorbing state of the EMC model. It implies $\text{Prob}(x(t)=0)=1$ as $t\to+\infty$, which in turn yields

$$\mathbb{E}_t(x)=0,\quad \mathbb{V}\text{ar}_t(x)=0,\quad \text{as}\quad t\ \to\ +\infty.$$

The probability distribution of EMC model and the corresponding expectation and variance are tough to obtain because of the complexity of the force function in (4.1). However, it is possible to make some qualitative moment analysis on the EMC model, especially on its expectation and variance. Denote $p_i(t)$ as the probability of $x(t)=i$ at time $t$ and similar to (3.5) and (3.8), the forward Kolmogorov equation of $p_i(t)$ is

$$\begin{cases}\dfrac{\mathrm{d}p_i(t)}{\mathrm{d}t}=F_{i-1}p_{i-1}(t)+H_{i+1}p_{i+1}(t)-(H_i+F_i)p_i(t),\quad i\geq 1,\\ \dfrac{\mathrm{d}p_0(t)}{\mathrm{d}t}=H_1p_1(t).\end{cases} \tag{4.4}$$

To simplify the calculation, we view $F(i)$ and $H(i)$ as quadratic polynomials as follows:

$$F_i=a_1i+a_2i^2,\quad H_i=b_1i+b_2i^2, \tag{4.5}$$

where

$$a_1=\big(\mathbb{P}_{\text{dist}}(n)P_{\text{out}}+V_{\text{m}}P_{\text{res}}\big)\mathbb{P}(\mathscr{C}),\quad a_2=-\frac{a_1}{N},\quad b_1=c_1r_1k_1,\quad b_2=c_2r_2k_2. \tag{4.6}$$

Based on (4.4), the differential equation of its probability generating function is given by

$$\frac{\partial\mathcal{P}(z,t)}{\partial t}=[(a_1+a_2)z-(b_1+b_2)](z-1)\frac{\partial\mathcal{P}(z,t)}{\partial z}+(a_2z-b_2)(z-1)z\frac{\partial^2\mathcal{P}(z,t)}{\partial z^2}, \tag{4.7}$$

where

$$\mathcal{P}(z,t)=\sum_{i=1}^{+\infty}z^iP_i(t).$$

Letting $z=e^\theta, \mathcal{P}(z,t)=M(\theta,t)$, then $\mathcal{P}$ and $M$ satisfy

$$\frac{\partial\mathcal{P}}{\partial z}=\frac{1}{z}\frac{\partial M}{\partial\theta},\quad \frac{\partial^2\mathcal{P}}{\partial z^2}=-\frac{1}{z^2}\frac{\partial M}{\partial\theta}+\frac{1}{z^2}\frac{\partial^2 M}{\partial\theta^2}.$$

Then from (4.7), the partial differential equation of $M$ is given by

$$\frac{\partial M(\theta,t)}{\partial t}=(1-e^{-\theta})\left[(a_1e^\theta-b_1)\frac{\partial M}{\partial\theta}+(a_2e^\theta-b_2)\frac{\partial^2 M}{\partial\theta^2}\right].$$

Through the property of the moment generating function, the differential equations of the first and second moments of $x(t)$ satisfy

$$\begin{cases}\dfrac{\mathrm{d}\mathbb{E}_t(x)}{\mathrm{d}t}=(a_1-b_1)\mathbb{E}_t(x)+(a_2-b_2)\mathbb{E}_t(x^2), & (4.8a)\\ \dfrac{\mathrm{d}\mathbb{E}_t(x^2)}{\mathrm{d}t}=(a_1+b_1)\mathbb{E}_t(x)+[2(a_1-b_1)+a_2+b_2]\mathbb{E}_t(x^2)+2(a_2-b_2)\mathbb{E}_t(x^3). & (4.8b)\end{cases}$$

Generally, we assume $\mathrm{Prob}(x(0)=k)=1, k\in\mathbb{Z}_+$, which further implies

$$\mathbb{E}_0(x)=k,\quad \mathbb{V}\mathrm{ar}_0(x)=0,\quad \mathbb{E}_0(x^n)=\mathbb{E}_0^n(x)=k^n. \tag{4.9}$$

If $a_1<b_1$, then $\mathbb{E}_t(x)$ will monotonously decrease to the absorbing state 0. If $a_1>b_1$, then from (4.8) and (4.9), if the initial value $k<K_c$, then $\mathbb{E}_t(x)$ will increase first on some small time interval $[0,t_0]$, but if $k>K_c$, it will decrease first on some time interval $[0,t_0]$, where $K_c:=(a_1-b_1)/(b_2-a_2)$. Besides, using $\mathbb{E}(x^2)\geq\mathbb{E}^2(x)$ and the Eq. (4.8a), we have

$$\frac{\mathrm{d}\mathbb{E}_t(x)}{\mathrm{d}t}\leq(a_1-b_1)\mathbb{E}_t(x)+(a_2-b_2)\mathrm{E}^2{}_t(x)=(a_1-b_1)\mathbb{E}_t(x)\left(1-\frac{1}{K_c}\mathbb{E}_t(x)\right).$$

It also implies the expectation of EMC model is less than the equilibrium of the deterministic logistic model, i.e. $\mathbb{E}_t(x)\leq K_c$. On the other hand, from the birth function $F_i$ in (4.5), we can see that $x(t)\leq N$, implying $\mathbb{E}_t(x)\leq N$. Thus, we have $\mathbb{E}_t(x)\leq\min\{K_c,N\}$. Besides, by multiplying $2\mathbb{E}_t(x)$ on both sides, the Eq. (4.8a) is changed as follows:

$$\frac{\mathrm{d}\mathbb{E}_t^2(x)}{\mathrm{d}t}=2(a_1-b_1)\mathbb{E}_t^2(x)+2(a_2-b_2)\mathbb{E}_t(x)\mathbb{E}_t(x^2),$$

and combining the Eq. (4.8b), we can obtain the differential equation of variance

$$\begin{aligned}\frac{\mathrm{d}\mathbb{V}\mathrm{ar}_t(x)}{\mathrm{d}t}=&\left[2(a_1-b_1)\left(1+\frac{\mathbb{E}_t(x)}{K_c}\right)+a_2+b_2\right]\mathbb{V}\mathrm{ar}_t(x)\\&+(a_1+b_1)\mathbb{E}_t(x)+(a_2+b_2)\mathbb{E}_t^2(x)+2(a_2-b_2)\left[\mathbb{E}_t(x^3)-\mathbb{E}_t^3(x)\right].\end{aligned}$$

From the boundedness of $\mathbb{E}_t(x)$ and the initial conditions of (4.9), there also exists a small $t_0$ such that $\mathbb{V}\mathrm{ar}_t(x)$ will increases over $[0,t_0]$. Furthermore, we can find that $\mathbb{E}_t(x^n)=0, n\in\mathbb{Z}^+$ is the solutions of (4.8) for all moments of the EMC model, which also has a good agreement with the classification of states. Finally, the results of qualitative moment analysis for the EMC model can be concluded in the following proposition.

**Proposition 4.1.** *If the EMC model meets the initial conditions* (4.9) *and* $k<K_c$*, then the expectation* $\mathbb{E}_t(x)$ *is nonnegative and bounded with* $\mathbb{E}_t(x)\leq\min\{K_c,N\}$*;* $\mathbb{E}_t(x)$ *and* $\mathbb{V}\mathrm{ar}_t(x)$ *will increase first at the early stage and ultimately decrease to absorbing state* 0*.*

### 4.3 Quasi-stationary probability distribution of EMC model

As we mentioned in the previous subsection, differing from the deterministic logistic model which has a globally asymptotically stable positive equilibrium, the EMC model will finally decline to the unique absorbing point, i.e. $p_0(t)=1$ as $t\to+\infty$. This also implies that the EMC model has no stationary probability distribution. But if the lasting time before absorption is quite long, there exists an approximate stationary distribution, i.e. $x(t)$ will randomly oscillate around the equilibrium $E^*:=K_c$ where the birth and death probabilities are almost equal. It becomes more obvious that $x(t)$ obeys a certain approximate distribution as the absorbing time gets longer and the approximate distribution is known as the quasi-stationary probability distribution depicting the probability distribution of $x(t)$ conditioned on non-extinction, denoted as $q_i(t)$ [2]. Thus, we have

$$q_i(t)=\frac{p_i(t)}{1-p_0(t)}.$$

Differentiating $q_i(t)$ with respect to $t$ and using the forward Kolmogorov equation in (4.4), we have

$$\frac{\mathrm{d}q_i}{\mathrm{d}t}=F_{i-1}q_{i-1}+H_{i+1}q_{i+1}-(H_i+F_i)q_i+H_1q_1q_i,\quad i=1,2,\ldots,N.$$

Generally, the last term in the above equation is quite small, thus the quasi-stationary distribution can be approximated by assuming $H_1q_1$ is close to 0. Subsequently, it can be expressed in the matrix form

$$\frac{dq}{dt}=\mathbb{Q}q, \tag{4.10}$$

where

$$\mathbb{Q}=\begin{pmatrix}-F_1 & H_2 & 0 & \cdots\\ F_1 & -F_2-H_2 & H_3 & \cdots\\ 0 & F_2 & -F_3-H_3 & \cdots\\ \vdots & \vdots & \vdots & \ddots\end{pmatrix}.$$

If there exists a stationary distribution $\pi=\{\pi_i\}$ for the new process (4.10), it is required to satisfy

$$q(t)\pi=\pi,$$

which implies that $Q\pi=0$ after differentiation. Thus, through solving the homogenous linear equation of $\pi$, we have the following results:

$$\pi_i=\prod_{k=1}^{i-1}\frac{F_k}{H_{k+1}}\pi_1,\quad \sum_{i=1}^{N}\pi_i=1. \tag{4.11}$$

Based on (4.11), the whole quasi-stationary probability distribution $\pi$ of the EMC model can be obtained.

### 4.4 Sustained chronicity risk and expected recovery time

We first introduce the concept of sustained chronicity risk in HBV infection. The previous subsection indicates that the stochastic process $x(t)$ will undergo a quasi-stationary distribution before the final absorption. Thus, the sustained chronicity risk $\mathbb{P}_{\rm c}(i)$ is defined as the probability that $x(t)$, starting from $x(0)=i$, arrives at quasi-steady state before final absorption. Considering that the quasi-stationary perturbation occurs around the probability equilibrium (the intersection of infection and immune force functions), we denote $n_e\triangleq[\min\{E_1^*,E_2^*\}]$, where $E_1^*,E_2^*$ are the intersections and $[\cdot]$ denotes the floor function. The sustained chronicity probability $\mathbb{P}_{\rm c}$ is given by the following conditional probability:

$$\mathbb{P}_{\rm c}(i)\triangleq\lim_{t\to+\infty}\text{Prob}\big(x(t)=0\,|\,\exists t'\in(0,t),x(t')=n_e,\text{ and }x_0=i\big),\quad i\in\mathbb{Z}_+.$$

Noticing if $i\geq n_e$, there always exists $\mathbb{P}_{\rm c}(i)=1$, since crossing $n_e$ is required for reaching 0. Thus, we only consider the case of $i\leq n_e$. $\mathbb{P}_{\rm c}(i)$ can be derived by recursive methods,

$$\mathbb{P}_{\rm c}(i)=F_i\Delta t\mathbb{P}_{\rm c}(i+1)+H_i\Delta t\mathbb{P}_{\rm c}(i-1)+[1-(F_i+H_i)\Delta t]\mathbb{P}_{\rm c}(i),\quad i<n_e. \tag{4.12}$$

Simplifying (4.12), we can obtain the following iterative equation:

$$\mathbb{P}_{\rm c}(i)=\mathcal{F}_i\mathbb{P}_{\rm c}(i+1)+\mathcal{H}_i\mathbb{P}_{\rm c}(i-1), \tag{4.13}$$

where $\mathcal{F}_i,\mathcal{H}_i$ are defined as (4.3) and its boundary conditions are

$$\mathbb{P}_{\rm c}(0)=0,\quad \mathbb{P}_{\rm c}(n_e)=1.$$

The analytical solutions of the iterative equation (4.13) is hard to obtained, but it is feasible to obtain its numerical solution by linear algebraic methods. Specially, (4.13) can be written as

$$\mathcal{H}_i\mathbb{P}_{\rm c}(i-1)-\mathbb{P}_{\rm c}(i)+\mathcal{F}_i\mathbb{P}_{\rm c}(i+1)=0,$$

and further expressed as matrix equation

$$\mathbb{M}\mathbb{P}_{\mathrm{c}}=\mathbf{0}, \tag{4.14}$$

where

$$\mathbb{M}=\begin{pmatrix} -1 & \mathcal{F}_1 & 0 & \cdots & 0 & 0 & 0 \\ \mathcal{H}_2 & -1 & \mathcal{F}_2 & \cdots & 0 & 0 & 0 \\ 0 & \mathcal{H}_3 & -1 & \cdots & 0 & 0 & 0 \\ \vdots & \vdots & \vdots & \ddots & \vdots & \vdots & \vdots \\ 0 & 0 & 0 & \cdots & -1 & \mathcal{F}_{n_e-2} & 0 \\ 0 & 0 & 0 & \cdots & \mathcal{H}_{n_e-1} & -1 & \mathcal{F}_{n_e-1} \end{pmatrix},$$

and $\mathbb{P}_{\mathrm{c}}=(\mathbb{P}_{\mathrm{c}}(1),\mathbb{P}_{\mathrm{c}}(2),\cdots,\mathbb{P}_{\mathrm{c}}(n_e))^\top, \mathbf{0}=(0,0,\cdots,0)^\top\in\mathbb{R}^{n_e}$.

Noticing $\mathrm{Rank}(\mathbb{M})=n_e-1$, thus Eq. (4.14) has a one-dimensional solution denoted as $\mathbb{P}_{\mathrm{c}}=\lambda\mathbb{P}_{\mathrm{e}}$, where $\lambda$ is an arbitrary real number and $\mathbb{P}_{\mathrm{e}}$ is the fundamental solution. From $\mathbb{P}_{\mathrm{c}}(n_e)=1$, we know that the solution $\mathbb{P}_{\mathrm{c}}$ is unique in $\mathbb{R}^{n_e}$. Therefore, by normalizing the last element $\mathbb{P}_{\mathrm{c}}(n_e)$, the numerical solution of $\mathbb{P}_{\mathrm{c}}$ can be obtained, and we have the following theorem.

**Theorem 4.1.** *The sustained chronicity risk $\mathbb{P}_{\mathrm{c}}$ in the EMC model is the solution of linear equation* (4.14) *after normalizing the last element of the one-dimensional fundamental solution $\mathbb{P}_e$.*

We next discuss the expected recovery time of HBV infection. The recovery time is defined as the first passage time of $x(t)$ reaching extinction and given by

$$\tau_i\triangleq\inf\{t\,|\,x(t)=0,x(0)=i\},\quad i=0,1,\ldots,N. \tag{4.15}$$

Noticing $\tau_i$ is a stop time, we define $T_i=\mathbb{E}(\tau_i)$ as the expected recovery time. Following the methods of (4.12), we can obtain the recursive equation about $T_i$, which is

$$T_i=F_i\Delta t(T_{i+1}+\Delta t)+H_i\Delta t(T_{i-1}+\Delta t)+\big(1-(F_i+H_i)\Delta t\big)(T_i+\Delta t). \tag{4.16}$$

Simplifying (4.16), we have

$$T_i=\frac{1}{F_i+H_i}+\frac{F_i}{F_i+H_i}T_{i+1}+\frac{H_i}{F_i+H_i}T_{i-1}. \tag{4.17}$$

Eq. (4.17) has two boundary conditions: $T_0=0$ from (4.15) and $F_N=0$ from (4.5) and (4.6). Based on the boundary conditions, we can calculate $T_i$. Particularily, the analytical expression of $T_i$ has been studied by Nisbet and Gurney ([2, Theorem 6.3], [27]), here we omit the derivation and present the conclusion directly.

**Theorem 4.2.** *The expected recovery time $T_i$ in the EMC model is the solution of Eq* (4.17)*, which is given by*

$$T_i=\begin{cases} \dfrac{1}{H_1}+\displaystyle\sum_{k=2}^{N}\frac{F_1\cdots F_{k-1}}{H_1\cdots H_k}, & i=1, \\ T_1+\displaystyle\sum_{s=1}^{i-1}\left[\frac{H_1\cdots H_s}{F_1\cdots F_s}\sum_{k=s+1}^{N}\frac{F_1\cdots F_{k-1}}{H_1\cdots H_k}\right], & i=2,\ldots,N. \end{cases} \tag{4.18}$$

# 5 Numerical validation

In this section, based on the numerical trajectory samples, we will validate the theoretical results of the three Markov models. Furthermore, the feasibility of EMC model with immune saturation is investigated as well.

## 5.1 Validation of CMC and DMC

This subsection will use the CMC and DMC models to numerically generate the colonization and diffusion processes of HBV particles in a single hepatic lobule. The colonization probability and the layer-wise infection probability distribution for the CMC model will be simulated and verified. Additionally, the DMC model with linear and logistic force functions will also be simulated and the moment analysis results will be verified.

According to the anatomy of hepatic lobule, the width of a single hepatic lobule is around 1 mm and a single hepatocyte is about 20-30 μm. Thus, the total layer size $n$ is approximated between 17 and 25. For convenience, we set $n=20$ and the four transition probabilities in Table 1 as

$$(P_N,P_C,P_0,P_1)=(0.1,0.02,0.01,0.87). \tag{5.1}$$

Using the CMC model, we generate 1000 trajectory samples in each numerical trial, count the amount of trajectory samples that finally reach the absorbing states $\{N,C,V\}$ and calculate their corresponding frequency in the 2000 trials. Moreover, the layer-wise colonization probability distribution in (2.9) can also be simulated and estimated by the CMC model. On the other hand, we can directly use the formulae in Propositions 2.1 and 2.2 to calculate the absorbing probability and the layer-wise colonization probability. The corresponding results of numerical estimation and theoretical calculation are shown in Figs. 3(a) and 3(b). The blue bar is the estimated frequency of each absorption with a standard deviation and the orange curve is the theoretical value. The results confirm that they have good consistency.

We next further implement the validation of the DMC model. According to the two transmission channels of HBV particles in vivo, we choose $P_{\rm cc}=0.12$, $P_{\rm cv}=0.88$ as the probabilities of the cell-to-cell and cell-to-virus transmission channels, and assume the hepatocytes capacity in a single lobule is $K=100$. By the DMC model, we respectively generate the infection diffusion process with the linear and logistic force functions. Figs. 3(c)/3(d) respectively shows 100 trajectory samples with linear/logistic force function. Both panels show the processes of the expectation $\mathbb{E}_t(x)$ increasing from 1 to 100 and the variance $\mathbb{V}\mathrm{ar}_t(x)$ increasing first and decreasing to 0, which has a good agreement with the theoretical results.

Besides, the probability distributions of $x(t)$ can be calculated by formula (3.6), which meanwhile yields $\mathbb{E}(x(t))$ and $\mathbb{V}\mathrm{ar}(x(t))$. Through numerous samplings, we find the DMC model with linear force function evolves more quickly than that with logistic force function. For better visualizations, we take the probability distribution at time $10,20,40$

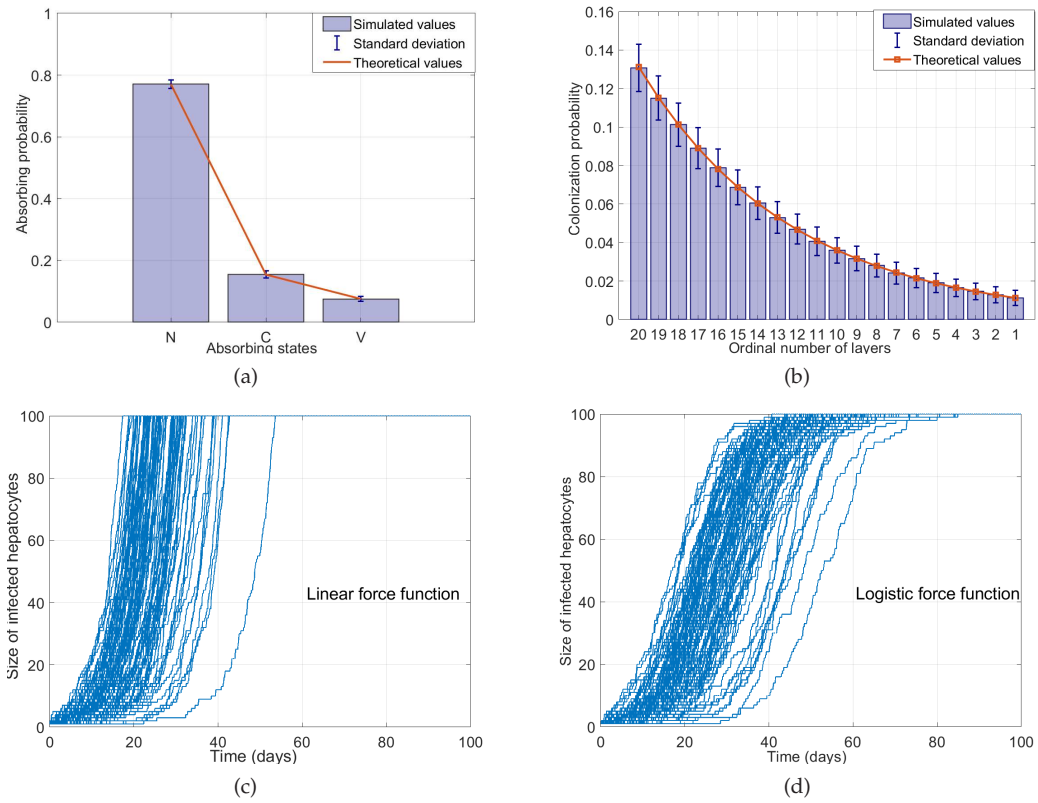


Figure 3: Illustrations for validating CMC and DMC models. (a) Absorbing probabilities of states $\{C,N,V\}$ in the CMC model with parameters from (5.1). (b) Layer-wise colonization probability distribution in an infected lobule with the maximum layers $n=20$. (c) The 100 trajectory samples of the DMC model with linear force function. (d) The 100 trajectory samples of the DMC model with logistic force function.

units of the DMC model with linear force function as examples, but take the distribution at later time 10,35,50 units with logistic force function as examples. The corresponding probability distributions with linear or logistic force functions are presented in Figs. 4(a)-4(c) and Figs. 4(d)-4(f), respectively. The illustrations indicate the results of theory and simulation have a good compatibility. Additionally, from the values of expectation and variance in left/right column of Fig. 4, we can observe that the expectation exhibits a monotonous increase under the conditions of the two force functions, yet the variance (standard deviation) exhibits a process of increasing first and decreasing to 0, which reflect a good agreement with the results in Theorem 3.2.

## 5.2 Validation of EMC model

This subsection will generate the trajectory samples of the EMC model and validate the theoretical results, including the quasi-stationary probability distribution, sustained chronicity risk and the expected recovery time for HBV infection.

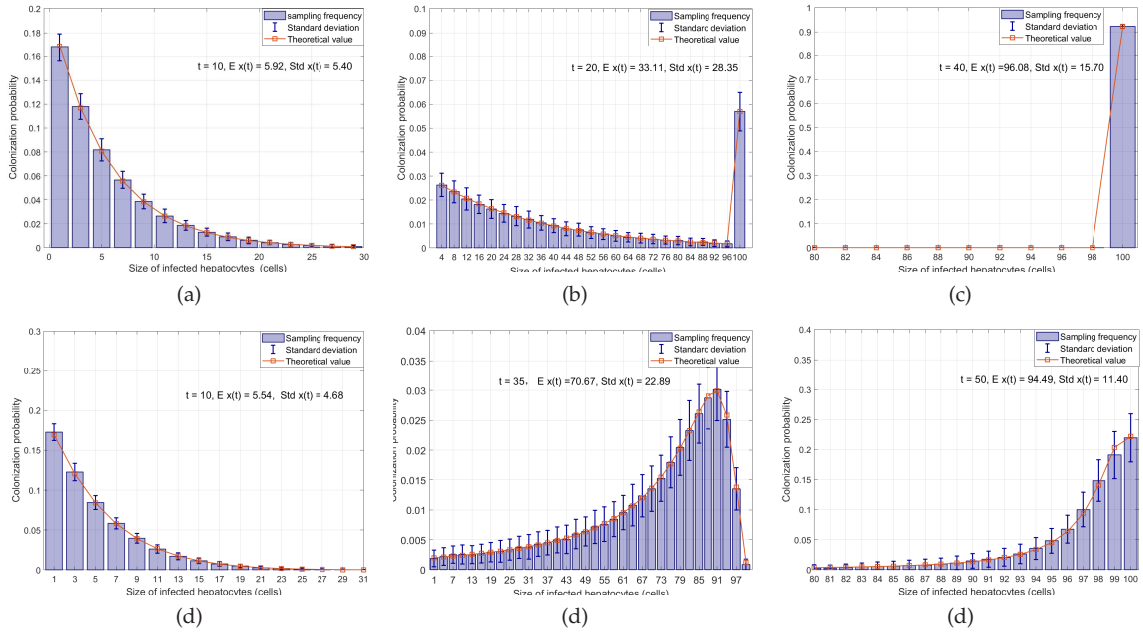


Figure 4: Probability distribution of DMC model with linear/logistic force function. Panels (a)-(c) are the probability distribution with linear force function at time 10,20,40 units. Panels (d)-(f) are the probability distribution with logistic force function at time 10,35,50 units. Both distributions of two growth patterns have a good compatibility with formula (3.6), and $\mathbb{E}(x(t))$ goes up and $\mathbb{V}\mathrm{ar}(x(t))$ increases before declines.

We first set the parameters in the EMC model. For the convenience of verifications, we set the total hepatic lobules as $N=100$, around 0.1% of the truth [3,21,26,35,40]. In the infection function $F_{\mathrm{sub}}$, following the basic parameters in (5.1) and the formula in (2.8), we have $\bar{P}_{\mathrm{C}}=0.0222$ and set $P_{\mathrm{out}}=0.1$. In the infection function $F_{\mathrm{cyc}}$, following (2.6), we have $\mathbb{P}(\mathscr{C})=0.157$, and set $V_{\mathrm{m}}=100$, $P_{\mathrm{res}}=5\%$. Thus, we have

$$F_i=F_{\mathrm{sub}}+F_{\mathrm{cyc}}=0.788i\left(1-\frac{i}{100}\right).$$

In the immune function $H_{\mathrm{nk}}$ and $H_{\mathrm{ctl}}$, it is reasonable to believe that the viral clearance rate of CTLs is higher than that of NK cells, and set $(r_1,r_2)=(0.1,0.3)$; the unit contact rates of both are the same value $k_1=k_2=0.03$; the concentration rate of NK cells is $c_1=50$ cells/ml in blood, and the concentration of CTLs are assumed as $c_2 i=5i$ (depending on $i$). Thus, we have

$$H_i=H_{\mathrm{nk}}+H_{\mathrm{ctl}}=0.15i+0.045i^2.$$

Based on the abovementioned $F_i$ and $H_i$, we generate 1000 trajectory samples of the EMC model with initial value $x(0)=1$. Fig. 5(a) displays 10 trajectory samples and the probability equilibrium is $n_e=12$; Fig. 5(b) presents 5 trajectory samples, which reflects that they all went extinct one after another; Fig. 5(c) shows the quasi-stationary probability density distribution of 1000 samples. Figs. 5(a) and 5(b) indicate the processes of

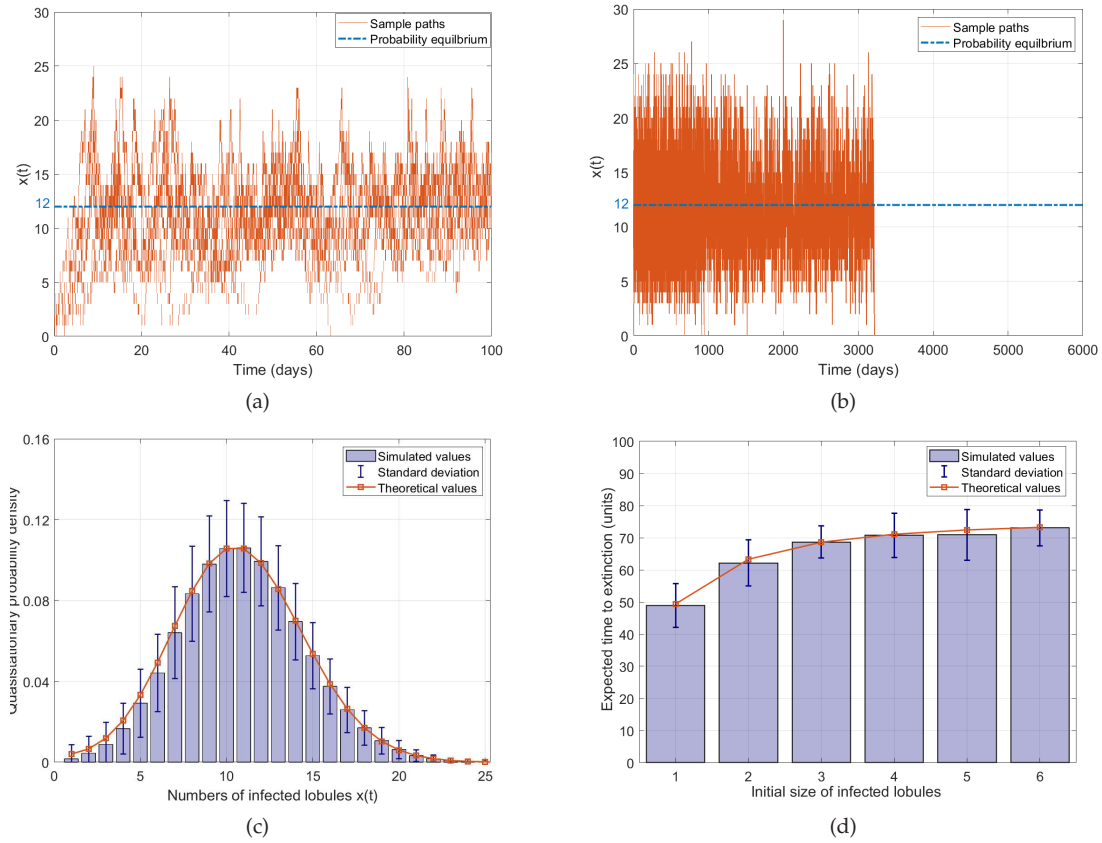


Figure 5: Trajectory samples and quasi-stationary probability distribution of EMC model. (a) A simulation of 10 trajectory samples of EMC model with initial value $x(0)=1$. (b) The extinction of 5 trajectory samples, implying extinction is inevitable. (c) The quasi-stationary probability distribution based on 1000 trajectory samples. (d) The first extinction time of EMC model. The blue bar with standard deviation is the simulated results from 1000 samples and the orange solid line with squares is calculated values.

$\mathbb{E}_t(x)$ and $\mathbb{V}\mathrm{ar}_t(x)$ increasing first and decreasing finally to 0; Fig. 5(c) indicates a good agreement between the numerical and theoretical results. The mutual support between them further implies the theoretical analyses and program algorithms are reliable.

We next simulate and verify the expected time to extinction of $x(t)$. Considering the sampling difficulty of extinction through simulation when the probability equilibrium $n_e$ is large, we increase the coefficient of concentration of CTL cell $c_2$ from 5 to 10, so that the immune intensity gets larger and the probability equilibrium $n_e$ decreases from 12 to 6, which is appropriate to demonstrate the expected time to extinction. Based on the previous simulation algorithms, we sample 200 trajectories with initial value $x(0)=1,2,\ldots,6$ over time $[0,2000]$, where all sample paths are observed extinction. The first extinction time of 200 samples with different initial values is collected and shown as the light blue bar with standard deviation in Fig. 5(d). For further comparison, the theoretical extinct time are shown in orange solid line with squares. The simulation results also have a good

consistency with the theoretical values calculated by (4.18), which further mutually supports the numerical algorithm for the simulation and the theoretical analysis.

### 5.3 EMC model with immune saturation

The immune function $H_i$ in (4.2) is initially assumed to be an unbounded quadratic function. However, the practical immune activity is constrained by the total immune resources available within-host. Therefore, it is more appropriate to model $H_i$ as a saturation function. Moreover, during drug therapy, biomarkers such as viral load and HBsAg often exhibit complex evolutionary dynamics. In addition to the typical monophasic rapid decay, various decline patterns – including biphasic decay, a flat second phase, triphasic decay, staircase decay, and rebound – have been observed [6, 20]. These observations further underscore the importance of incorporating immune saturation effects into the EMC model. Motivated by the viewpoints above, we promote EMC model to include the immune saturation effects, which is named as EMCS model.

To capture the saturation effect with an upper bound in immune activity, we incorporate a Hill function into the immune function $H_i$. As a result, the innate immune function $H_{\text{nk}}$ and the specific immune function $H_{\text{ctl}}$ are formulated as follows:

$$H_{\text{nk}}(i)=e_1\bar{s}_1\frac{i^{m_1}}{c_1^{n_1}+i^{n_1}},\quad H_{\text{ctl}}(i)=e_2\bar{s}_2\frac{i^{m_2}}{c_2^{n_2}+i^{n_2}},\quad m_i\le n_i,\quad i=1,2, \tag{5.2}$$

where $\bar{s}_i, c_i, e_i\ (i=1,2)$ are positive constants denoting the maximum immune clearance rate, half-saturation value and immune efficacy, respectively. The exponents $m_i$ and $n_i$ $(i=1,2)$ are the shape parameters that reflect the dependence on the infected lobules $i$. To ensure a linear relationship between $H_{\text{nk}}$ and $i$ near $i=0$, we set $m_1=n_1=1$. Furthermore, to capture the saturation behavior of the specific immune function $H_{ctl}$, we let $m_2=n_2=k\,(k>1)$. For notational convenience, denote $s_i=e_i\bar{s}_i\ (i=1,2)$, as the effective saturation value. From (5.2), the total immune function $H_i$ contributed by innate and specific immunity is given by

$$H_i^s=s_1\frac{i}{c_1+i}+s_2\frac{i^k}{c_2^k+i^k},$$

satisfying $H_i^s\to s_1+s_2$ as $t\to+\infty$.

Based on the theoretical results and numerical algorithm on the EMC model, we conduct preliminary numerical simulations of the EMCS model using the infection function $F_i=ri(1-i/500)$, $r\in[0.12,0.2]$ and set the parameters $(s_1,s_2,c_1,c_2,k)=(26.4,7.5,177,78,5)$ in $H_i^s$. Fig. 6(a) illustrates the intersection patterns between the infection and immune functions. It reveals that the saturated immune function $H_i^s$ can exhibit multiple intersections with the infection function as the infection rate $r$ varies, suggesting the potential for complex dynamical behavior. Fig. 6(b) shows the landscape of the quasi-stationary probability distribution over $r\in[0.12,0.2]$. Figs. 6(c)-6(f) show trajectory samples corresponding to the values of $r$ marked in panel (a), from bottom to top. The numerical results

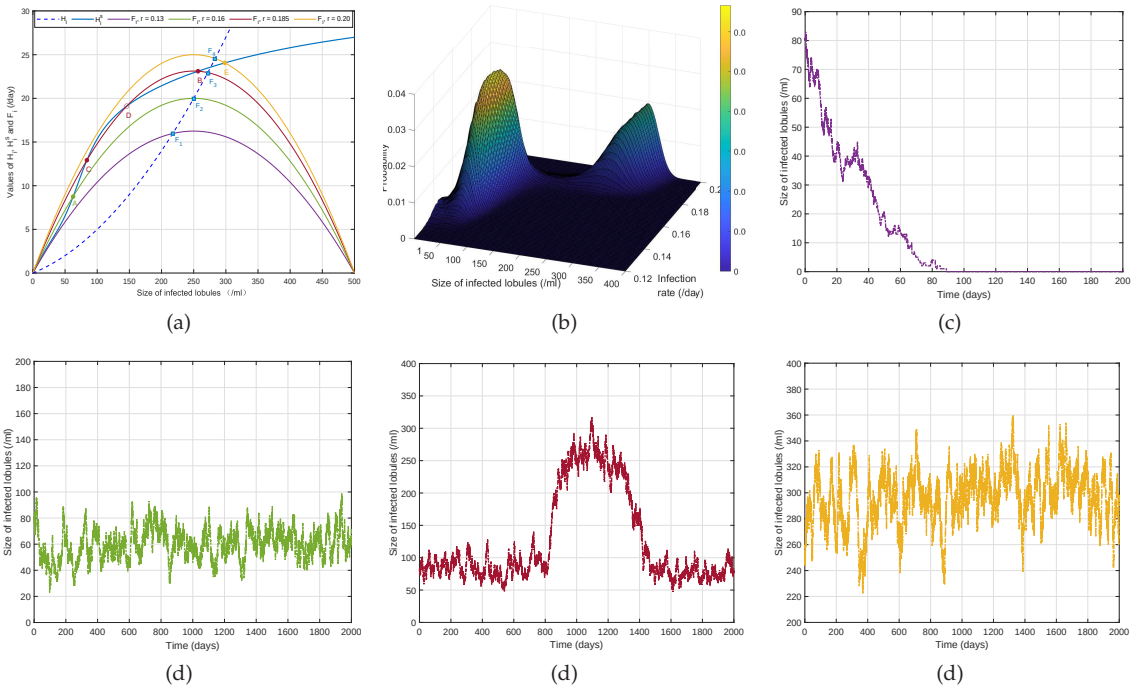


Figure 6: Illustrations of the EMCS model with varying infection rate $r$. (a) The blue dashed and solid lines represent the original quadratic immune function and the modified saturated immune function, respectively. The remaining curves depict the infection function $F_i$ with different $r$. (b) Landscape of the quasi-stationary probability distribution. (c)-(f) Trajectory samples of the EMCS model corresponding to the values of $r$ in panel (a), from bottom to top.

demonstrate that the EMCS model can reproduce not only direct decay and monophasic perturbation, but also biphasic oscillations and low/high single-peak perturbations. This indicates that incorporating immune saturation can indeed enrich the dynamic patterns observed in HBV infection, which is worth further verification by combining clinical data in the future.

## 6 Discussion

HBV infection within-host is a complex interaction among virus, hepatocytes and the immune system. A novel Markov modeling framework is established to elucidate the infection process, providing mathematical insights and treatment guidance. First, a CMC model based on the tissue structure of hepatic lobules is proposed to describe viral colonization. Using this model, the colonization probability and layer-wise infection distribution are analyzed. From Proposition 2.2 and Fig. 3(b), we can conclude that most infected hepatocytes are located in the outer layers of the hepatic lobules. Considering that the majority of cell division and proliferation occurs in the middle-layer hepatocytes [21,38], shortening the turnover time of hepatocytes may have a positive impact on

the elimination of early-stage infection. Then, a DMC model is introduced to represent the spread of infected hepatocytes within an infected lobule during early infection. The expectation and variance of the model solutions are qualitatively examined under linear or logistic growth assumptions. The results indicate that a linear force function is suitable to mimic the early diffusion process and a logistic force function is suitable to mimic the late diffusion process. Subsequently, an EMC model is developed to capture the dynamic evolution of infected lobules across the liver, with analytical expressions derived for the quasi-stationary distribution, sustained chronic risk, and expected recovery time. Finally, numerical verifications for all three Markov models strongly support the theoretical analyses, and based on these simulations, a preliminary numerical investigation on the EMCS model is conducted to reveal the necessity of immune saturation effect.

Although the modeling frameworks has well-fitting outcomes, several aspects of the current Markov framework require further improvement. The infection function $F_i$ in (4.2) connects the DMC and EMC models, unifying the three-model framework. In practice, estimating the mean viral load $V_m$ in $F_{\text{cyc}}$ and the probability $P_{\text{out}}$ in $F_{\text{sub}}$ remains practically challenging, requiring new estimation methods. Furthermore, complex dynamical patterns in HBV biomarkers – often associated with immune mechanisms such as $CD8^+$ T cell exhaustion – are frequently observed during chronic hepatitis B therapy [6, 20]. Although the introduction of immune saturation in this study enhances the EMC model's ability to reflect HBV infection dynamics, a more comprehensive representation might be achieved by allowing $m_i < n_i$ $(i = 1,2)$ in (5.2). This adjustment may potentially capture both immune saturation and exhaustion simultaneously, which is also worth further investigation in the future.

## Acknowledgments

We are very grateful to two anonymous reviewers for the valuable comments and suggestions.

This work was supported by the National Natural Science Foundation of China (Grant Nos. 12571546 (K. Wang), 12171396 (K. Wang), 12471460 (J. Wang)).

### References

[1] M. A. Ali, S. A. Means, H. Ho, and J. Heffernan, *Global sensitivity analysis of a single-cell HBV model for viral dynamics in the liver*, Infect. Dis. Model., 6:1220–1235, 2021.
[2] L. J. Allen, *An Introduction to Stochastic Process with Applications to Biology*, CRC Press, 2010.
[3] E. M. Andersson, *In the zone of liver proliferation*, Science, 371:887–888, 2012.
[4] S. M. Ciupe, R. M. Ribeiro, P. W. Nelson, and A. S. Perelson, *Modeling the mechanisms of acute hepatitis B virus infection*, J. Theor. Biol., 247:23–35, 2007.
[5] R. P. Cunningham, W. S. Kang, and N. P. Shliom, *Location matters: Cellular heterogeneity in the hepatic lobule and hepatocellular carcinoma*, Am. J. Physiol. - Gastrointest. Liver Physiol., 324(4):G245–G249, 2023.

[6] H. Dahari, E. Shudo, R. M. Ribeiro, and A. S. Perelson, *Modeling complex decay profiles of hepatitis B virus during antiviral therapy*, Hepatology, 49:32–38, 2009.
[7] S. J. Farlow, *Partial Differential Equations for Scientists and Engineers*, John Wiley and Sons, 1982.
[8] S. Foko, *Dynamical analysis of a general delayed HBV infection model with capsids and adaptive immune response in presence of exposed infected hepatocytes*, J. Math. Biol., 88:75, 2024.
[9] M. G. Ghany and E. C. Doo, *Antiviral resistence and hepatitis B therapy*, Hepatology, 49:174–184, 2009.
[10] A. Goyal, L. E. Liao, and A. S. Perelson, *Within-host mathematical models of hepatitis B virus infection: Past, present, and future*, Curr. Opin. Syst. Biol., 18:27–35, 2019.
[11] A. Goyal and J. M. Muarry, *Modelling the impact of cell-to-cell transmission in hepatitis B virus*, PLoS One, 11:e0161978, 2016.
[12] A. M. Herz, S. Bonhoeffer, R. M. Anderson, R. M. May, and M. A. Nowak, *Viral dynamics in vivo: Limitations on estimates of intracellular delay and virus decay*, Proc. Natl. Acad. Sci. USA, 93:7247–7251, 1996.
[13] J. H. Hoofnagle, E. Doo, T. J. Liang, R. Fleischer, and A. S. Lok, *Manegement of hepatitis B: Summary of a clinical research workshop*, Hepatology, 45:1056–1075, 2007.
[14] A. Jindal, M. Kumar, and S. K. Sarin, *Management of acute hepatitis B and reactivation of hepatitis B*, Liver Int., 33:164–175, 2013.
[15] F. John, *Partial Differential Equations*, Springer-Verlag, 1975.
[16] D. Kang, G. Hong, S. An, I. Jang, W.-S. Yun, J.-H. Shim, and S. Jin, *Bioprinting of multiscaled hepatic lobules within a highly vascularized construct*, Small, 16:1905505, 2020.
[17] K. Kitagawa et al., *Multiscale modeling of HBV infection integrating intra- and intercellular viral propagation to analyze extracellular viral markers*, PLoS Comput. Biol., 20:e1011238, 2024.
[18] A. M. Lam, S. Ren, C. Espiritu, M. Kelly, V. Lau, L. Zheng, G.D. Hartman, O. A. Flores, and K. Klumpp, *Hepatitis B virus capsid modulators, but not nucleoside analogs, inhibit the production of extracellular pregenomic RNA and spliced RNA variants*, Antimicrob. Agents Chemother., 61(8):e00680-17, 2017.
[19] M. L. Li and J. Zu, *The review of differential equation models of HBV infection dynamics*, J. Virol. Methods, 266:103–113, 2019.
[20] Y. F. Liaw, J. H. Kao, T. Piratvisuth, and H. L. Chan, *Asian-Pacific consensus statement on the management of chronic hepatitis B: A 2012 update*, Hepatol. Int., 6:531–561, 2012.
[21] Z. Liu, M. Takeuchi, M. Nakajima, C. Hu, Y. Hasegawa, Q. Huang, and T. Fukuda, *Three-dimensional hepatic lobule-like tissue construts using cell-microcapsule technology*, Acta Biomater., 50:178–187, 2017.
[22] A. F. Lok and B. J. McMahon, *Chronic hepatitis B*, Hepatology, 45:507–539, 2007.
[23] A. S. Lok, F. Zoulim, G. Dusheiko, and M. G. Ghany, *Hepatitis B cure: From discovery to regulatory approval*, J. Hepatol., 67:847–861, 2017.
[24] J. M. Murray and A. Goyal, *In silico single cell dynamics of hepatitis B virus infection and clearance.*, J. Theor. Biol., 366:91–102, 2015.
[25] J. M. Murray, S. F. Wieland, R. H. Purcell, and F. V. Chisari, *Dynamics of hepatitis B virus clearance in chimpanzees*, Proc. Natl. Acad. Sci. USA, 102:17780–17785, 2005.
[26] F. H. Netter, *Atlas of Human Anatomy*, Elsevier, 2019.
[27] R. M. Nisbet and W. S. Gurney, *Modelling Fluctuating Populations*, John Wiley and Sons, 1982.
[28] M. A. Nowak and C. M. Bangham, *Population dynamics of immune responses to persistent viruses*, Science, 272:74–79, 1996.
[29] M. A. Nowak, S. Bonhoeffer, A. M. Hill, R. Boehme, and H. C. Thomas, *Viral dynamics in*

*hepatitis B virus infection*, Proc. Natl. Acad. Sci. USA, 93:4398–4402, 1996.
[30] A. M. Rappaport, *The microcirculatory hepatic unit*, Microvasc. Res., 6:212–224, 1973.
[31] J. Rodés, J. P. Benhamou, A. T. Blei, J. Reichen, and M. Rizetto, *Textbook of Hepatology: From Basic Science to Clinical Practice*, Black Well Publishing, 2007.
[32] W. A. Seto, Y. R. Lo, J. M. Pawlotsky, and M. F. Yuen, *Chronic hepatitis B virus infection*, Lancet, 392:2313–2324, 2018.
[33] C. M. Séverine, M. Grégory, C. Dominique, and D. Chantal, *Polyploidy and liver proliferation: Central role of insulin signaling*, Cell Cycle, 9:460–466, 2010.
[34] The Lancet, *Towards elimination of viral hepatitis by 2030*, Lancet, 388:308, 2016.
[35] E. Trefts, M. Gannon, and D. Wasserman, *The liver*, Curr. Biol., 27:1141–1155, 2017.
[36] S. Urban, A. Schulze, M. Dandri, and J. Petersen, *The replication cycle of hepatitis B virus*, J. Hepatol., 52:282–284, 2010.
[37] K. F. Wang, W. T. Tan, Y. Z. Tang, and G. H. Deng, *Numerical diagnoses of superinfection in chronic hepatitis B viral dynamics*, Intervirology, 54:349–356, 2011.
[38] Y. L. Wei et al., *Liver homeostasis is maintained by midlobular zone 2 hepatocytes*, Science, 371(6532):eabb1625, 2021.
[39] World Health Organization, *Hepatitis B*, `https://www.who.int/news-room/fact-sheets/detail/hepatitis-b`.
[40] J. Y. Yang et al., *Preliminary exploration of architecture of human hepatic functional unit*, Journal of Third Military Medical University, China, 43:1713–1719, 2021. (In Chinese)
[41] S. Yapali, N. Talaat, and A. S. Lok, *Management of hepatitis B: Our practice and how it relates to the guidlines*, Clin. Gastroenterol. Hepatol., 12:16–26, 2014.
[42] M. F. Yuen et al., *Safety, pharmacokinetics, and antiviral effects of ABI-H0731, a hepatitis B virus core inhibitor: A randomised, placebo-controlled phase 1 trial*, Lancet Gastroenterol., 5:152–166, 2020.
[43] M. P. Zegers and D. Hoekstra, *Mechanisms and functional features of polarized membrane traffic in epithelial and hepatic cells*, Biochem. J., 336:257–269, 1998.
[44] P. Zhong, L. M. Agosto, J. B. Munro, and W. Mothes, *Cell-to-cell transmission of viruses*, Curr. Opin. Virol., 3:44–50, 2013.